ISSN 0021-3640, JETP Letters, 2023, Vol. 117, No. 7, pp. 492–497. © The Author(s), 2023. This article is an open access publication.
Russian Text © The Author(s), 2023, published in Pis'ma v Zhurnal Eksperimental'noi i Teoreticheskoi Fiziki, 2023, Vol. 117, No. 7, pp. 492–497.

FIELDS, PARTICLES, AND NUCLEI

Form Factor in Transition Radiation from Hollow Beams

D. Yu. Sergeeva[a] (ORCID: 0000-0002-9749-4697) and A. A. Tishchenko[a, b, *] (ORCID: 0000-0002-1963-4973)

[a] *National Research Nuclear University MEPhI (Moscow Engineering Physics Institute), Moscow, 115409 Russia*

[b] *International Scientific Educational Radiation Physics Laboratory, Belgorod National Research University, Belgorod, 308034 Russia*

**e-mail: tishchenko@mephi.ru*

Received February 26, 2023; revised March 3, 2023; accepted March 3, 2023

The form factor of a hollow electron beam for transition radiation has been calculated. It has been shown that the characteristics of coherent radiation are significantly different for conventional solid and hollow beams. Numerical estimates have been obtained for terahertz radiation frequencies and relativistic energies of electrons.

DOI: 10.1134/S0021364023600544

1. INTRODUCTION

Hollow electron beams, i.e., beams with a ring cross section, are currently under intensive study. In particular, the authors of [1–3] proposed to use hollow electron beams to collimate intense main proton or ion beams at the CERN Large Hadron Collider. Electron beams are introduced in the collimation system in order to clean the halo, whereas the main beam circulates inside a hollow electron beam. The hollow electron beam resonantly excites the tails of the main beam, whereas the core of the main beam remains unperturbed. Such devices are called hollow electron lenses. The cleaning of the halo is relevant because of the performed works to increase the total fluence at the Large Hadron Collider by an order of magnitude.

The use of hollow electron lenses necessarily requires the diagnostics of the transverse dimensions of the main and hollow electron beams. One of the actively developed ideas is to use the fluorescence of gas [4]. An advantage of this method is that measurements hardly distort the properties of a beam. Since the method is novel, optical transition radiation is used for its cross test. Optical transition monitors are successfully used to measure the transverse profile of electron beams at accelerators [5–7].

The acceleration of charged particles also is a promising field where hollow beams of charged particles are used. Positrons can be accelerated to high energies in wakefields generated by hollow electron beams moving in a plasma. This possibility was confirmed by the computer simulation of the generation of wakefields and the dynamics of hollow electron beams [8–10].

It is also important to study the dynamics of hollow beams and the characteristics of radiation that is generated by them for the actively developed physics of particles with a nonzero orbital angular momentum (twisted electrons) [11, 12] because the distribution functions describing twisted electrons or electron beams are similar in the classical approach to the electron distribution function in the hollow beam.

Only the single-electron approach is used in most studies of hollow beams. The difference of the multielectron approach from the single-electron one is briefly in the inclusion of the form factor of the beam, which depends on the shape, density, and dimensions of the beam and on the electron distribution function in the beam $f(\mathbf{r})$. In [13, 14], we show that the form factor depends on the type of radiation. In this work, we calculate the form factor of the hollow beam for transition radiation; see Fig. 1.

2. CONVENTIONAL APPROACH

The form factor is long known for synchrotron and some other types of radiation but mainly in the case of the Gaussian or uniform electron distribution in a beam [15–17]. It is noteworthy that known form factors are often used incorrectly; moreover, the notion of form factor is sometimes inapplicable; for details, see [14, 18].

The intensity of most types of radiation can be represented in the form

$$I_N = I_1 F, \tag{1}$$

where I_1 is the intensity of radiation from a single electron and F is the form factor of the beam. The intensity can be defined as, e.g., the angular and frequency distribution of the emitted energy [13] or radiation power [19]. In the case of a large number of electrons in a

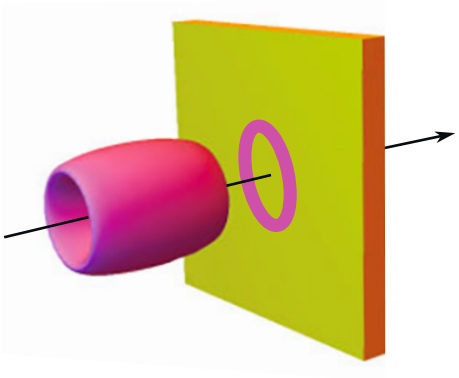

Fig. 1. (Color online) Hollow electron beam shown in rose intersects the target given in green and generates transition radiation.

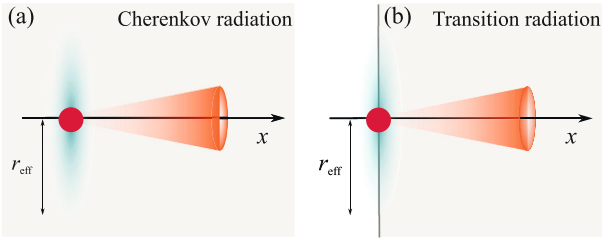

Fig. 2. (Color online) Electron marked in red excites (a) Cherenkov radiation moving in the medium and (b) transition radiation crossing the interface between two media indicated by the vertical line; r_{eff} is the effective relaxation radius of the electron field shown in blue.

beam $N \gg 1$, the form factor can be expressed by the formula

$$F = NF_{\text{inc}} + N^2F_{\text{coh}}. \tag{2}$$

Here, F_{coh} and F_{inc} are the coherent and incoherent form factors, respectively. A particular form of F_{coh} and F_{inc} depends on the type of radiation.

We consider polarization radiation generated by a charged particle interacting with an infinite amorphous medium, i.e., a medium where the distance from its edges to an electron perpendicular to its trajectory is much larger than the effective radius of relaxation of the field of the moving electron $r_{\text{eff}} \approx \gamma\beta\lambda/2\pi$. Here, γ is the Lorentz factor of the electron, λ is the radiation wavelength, and $\beta = v/c$, where v is the velocity of the electron and c is the speed of light in vacuum. In other words, the medium can be treated as infinite if the electron is "insensitive" to the edges of the medium (see Fig. 2). This treatment is applicable to transition radiation, Cherenkov radiation, and parametric X-ray radiation. The source of these types of radiation is the material of a target, which is dynamically polarized under the action of the field of the moving relativistic electron. In this case, the velocity of the electron can be considered constant when the kinetic energy of the electron is much larger than the energy transferred to radiation.

The incoherent form factor for such types of radiation is $F_{\text{inc}} = 1$ (see, e.g., [20]) because all electrons make the same contribution to the polarization of the medium; i.e., the transverse position of an electron does not affect the characteristics of radiation [14]. The coherent form factor for transition radiation is calculated by the formula [13, 14]

$$F_{\text{coh}} = \left|\int d\mathbf{r} f(\mathbf{r}) e^{-i\frac{\omega}{v}x} e^{-ik_y y} e^{-ik_z z}\right|^2, \tag{3}$$

where $f(\mathbf{r})$ is the normalized electron distribution function in the beam, $\mathbf{r}$ is the position vector of the electron with respect to the center of the beam, $\omega = 2\pi c/\lambda$ is the frequency of radiation, and $\mathbf{k} = (k_x, k_y, k_z)$ is the wave vector of radiation. Formula (3) is obtained under the assumption that all electrons move at a constant velocity $\mathbf{v}$ along the OX axis; i.e., the angular divergence of the beam, as well as the energy spread in it, is disregarded. Formula (3) can be obtained by calculating the radiation intensity of radiation for all electrons in terms of the corresponding field and by averaging the result over the positions of all electrons.

3. HOLLOW BEAM

We consider the beam with the Gaussian distribution of electrons in the longitudinal direction parallel to the velocity; the beam is hollow in the transverse direction. Let the longitudinal and transverse components of the position vector of the electron be independent. Then, neglecting correlations in the beam and assuming that the positions of electrons are independent of the positions of their neighbors, we can represent the distribution function $f(\mathbf{r})$ in the form

$$f(\mathbf{r}) = f_{\text{long}}(x) f_{\text{tr}}(y, z), \tag{4}$$

where $f_{\text{long}}(x)$ and $f_{\text{tr}}(y, z)$ are the longitudinal and transverse distribution functions, respectively. The longitudinal profile of the beam determines the explicit form of the corresponding multiplier in the form factor and can be arbitrary.

The distribution functions for the beam under consideration can be written in cylindrical coordinates in the form

$$f_{\text{long}}(x) = (\sigma_x\sqrt{\pi})^{-1} \exp[-x^2/\sigma_x^2], \tag{5}$$

where σ_x is the characteristic longitudinal dimension of the beam;

$$f_{\text{tr}}(R, \varphi) = A \exp[-(R - r_0)^2/\sigma_{\text{tr}}^2], \tag{6}$$

where R and φ are the cylindrical coordinates introduced through the relations $y = R\cos\varphi$ and $z = R\sin\varphi$, r_0 is the radius of the hollow beam, σ_{tr} is the thickness of the beam ring, and A is the normalization coefficient given by the expression

$$A = (\pi\sigma_{tr}^2)^{-1}(\sqrt{\pi}\mu[1+\mathrm{erf}(\mu)] + e^{-\mu^2})^{-1}. \quad (7)$$

Here, $\mu = r_0/\sigma_{tr}$ and $\mathrm{erf}(\mu)$ is the error function specified by the formula

$$\mathrm{erf}(\mu) = \frac{2}{\sqrt{\pi}}\int_0^{\mu} dt\exp(-t^2). \quad (8)$$

In this work, we ignore the rotation of electrons inside the beam and the orbital angular momentum of electrons. It is important to take into account the orbital angular momentum of electrons, e.g., when considering quantum packets with a nonzero orbital angular momentum. The inclusion of these effects not only changes the description of the structure of the beam but also requires the recalculation of the intensity of transition radiation from one electron (see, e.g., [11]). Figure 3 shows two transverse distribution functions.

The substitution of the distribution functions (5) and (6) into Eq. (3) gives the following expression for the coherent form factor of the hollow beam:

$$F_{coh} = F_{long}F_{tr}. \quad (9)$$

Here, F_{long} and F_{tr} are the longitudinal and transverse coherent form factors, respectively, given by the expressions

$$F_{long} = \exp(-\omega^2\sigma_x^2/(2v^2)), \quad (10)$$

$$F_{tr} = 4\pi^2A^2|L|^2. \quad (11)$$

Here,

$$L = \int_0^{+\infty} dR R e^{-\frac{(R-r_0)^2}{\sigma_{tr}^2}} J_0(Rk_{tr}), \quad (12)$$

where J_0 is the zeroth-order Bessel function and $k_{tr} = \sqrt{k_y^2 + k_z^2}$. Substituting the known expansion [21]

$$J_0(Rk_{tr}) = \sum_{s=0}^{+\infty}(-1)^s\frac{(Rk_{tr})^{2s}}{2^{2s}(s!)^2} \quad (13)$$

into Eq. (12), we obtain

$$L = e^{-\mu^2}\sum_{s=0}^{+\infty}(-1)^s\frac{k_{tr}^{2s}\sigma_{tr}^{2(s+1)}}{2^{2s+1}(s!)^2}G_s, \quad (14)$$

where

$$G_s = \Gamma(1+s)\Phi(s+1,1/2;\mu^2) + 2\mu\Gamma(s+3/2)\Phi(s+3/2,3/2;\mu^2). \quad (15)$$

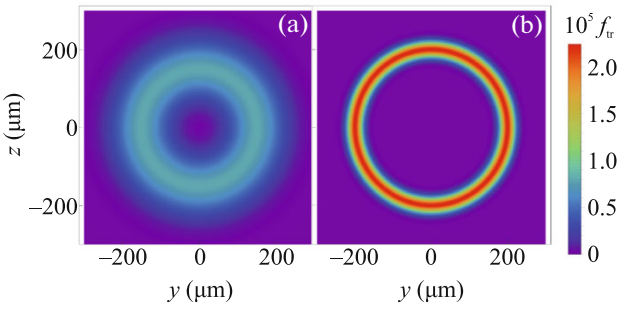

Fig. 3. (Color online) Transverse profile of the hollow beam with (a) $r_0 = 150$ μm and $\sigma_{tr} = 75$ μm ($\mu = 2$) and (b) $r_0 = 200$ μm and $\sigma_{tr} = 20$ μm ($\mu = 0$).

Here, $\Phi \equiv {}_1F_1$ is the confluent hypergeometric function and Γ is the gamma function. The final expression for the transverse coherent form factor of the hollow electron beam has the form

$$F_{tr} = \pi^2\sigma_{tr}^4A^2e^{-2\mu^2}\left|\sum_{s=0}^{+\infty}(-1)^s\frac{\sigma_{tr}^{2s}k_{tr}^{2s}}{2^{2s}(s!)^2}G_s\right|^2. \quad (16)$$

According to this expression, the form factor depends on the radiation observation angle. In other words, the effect of the beam shape on the characteristics of radiation depends on the radiation propagation direction.

Expression (16) applied to an electron beam with the conventional Gaussian transverse distribution, i.e., with $r_0 = 0$ or $\mu = 0$, has the form

$$F_{tr} = \exp(-\sigma_{tr}^2k_{tr}^2/2) \quad (r_0 = 0, \mu = 0). \quad (17)$$

This expression coincides with a classical expression (see, e.g., [20]).

Using known recurrence relations for confluent hypergeometric functions, Eq. (14) can be reduced to the form

$$L = \frac{\sigma_{tr}^2}{2}e^{-\mu^2}\sqrt{\pi}\sum_{s=0}^{+\infty}\left(\frac{\mu^{2s}\Phi[s+1,1,-(\sigma_{tr}k_{tr}/2)^2]}{\Gamma(s+1/2)} + \mu^{2s+1}\Phi[s+3/2,1,-(\sigma_{tr}k_{tr}/2)^2]/\Gamma(s+1)\right). \quad (18)$$

Here, the first confluent hypergeometric function can be represented in the form

$$\Phi\left[s+1,1,-\frac{\sigma_{tr}^2k_{tr}^2}{4}\right] = e^{-\frac{\sigma_{tr}^2k_{tr}^2}{4}}\sum_{m=0}^{s}\frac{(-1)^m s!(\sigma_{tr}k_{tr})^{2m}}{2^{2m}(m!)^2(s-m)!}. \quad (19)$$

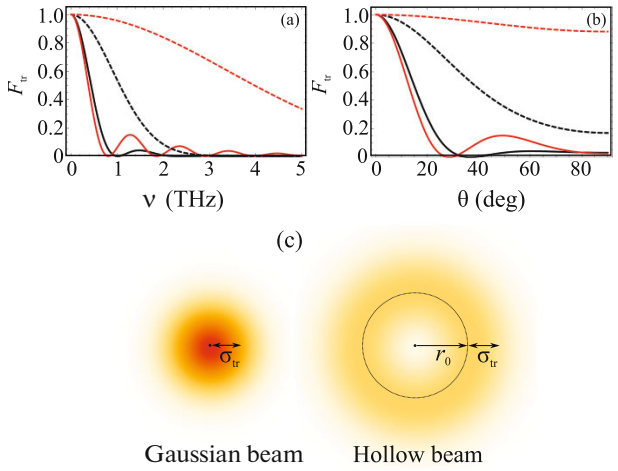

Fig. 4. (Color online) Transverse form factor versus (a) the frequency of radiation at $\theta = 45°$ and (b) the radiation observation angle at $\nu = 1.2$ THz for the (solid lines) hollow and (dashed lines) Gaussian beams at $\gamma = 16$ and (black solid line) $\mu = 2$ and $\sigma_{tr} = 75$ μm, (red solid line) $\mu = 10$ and $\sigma_{tr} = 20$ μm, (black dashed line) $\mu = 0$ and $\sigma_{tr} = 75$ μm, and (red dashed line) $\mu = 0$ and $\sigma_{tr} = 20$ μm. (c) Profiles of the Gaussian and hollow beams with the same standard deviation σ_{tr}.

In order to transform the second term in Eq. (18), we use the formula obtained in [22]. Simple transformations give

$$\Phi\left[s+3/2,1,-\left(\frac{\sigma_{tr}k_{tr}}{2}\right)^2\right] = e^{-\frac{\sigma_{tr}^2k_{tr}^2}{8}}\left(I_0\left[\frac{\sigma_{tr}^2k_{tr}^2}{8}\right]\right. \\ \left. + 2\sum_{m=1}^{+\infty}{}_3F_2\left(-m,m,s+\frac{3}{2};1,\frac{1}{2};1\right)I_m\left[\frac{\sigma_{tr}^2k_{tr}^2}{8}\right]\right), \quad (20)$$

where ${}_3F_2$ is the generalized hypergeometric function, which in this case is independent of the parameters of the problem and is a numerical coefficient and I_0 and I_m are the modified Bessel functions. We note that recurrence relations reduce I_m to a combination of the functions I_0 and I_1.

The final expression for the transverse form factor (16) has the form

$$F_{tr} = \pi^3A^2\sigma_{tr}^4e^{-2\mu^2}e^{-\frac{\sigma_{tr}^2k_{tr}^2}{4}}\left|\mu e^{\mu^2}I_0\left[\frac{\sigma_{tr}^2k_{tr}^2}{8}\right]\right. \\ \left. + e^{-\frac{\sigma_{tr}^2k_{tr}^2}{8}}\sum_{s=0}^{+\infty}\frac{\mu^{2s}s!}{\Gamma(s+1/2)}\sum_{m=0}^{s}\frac{(-1)^m(\sigma_{tr}k_{tr}/2)^{2m}}{(m!)^2(s-m)!}\right. \\ \left. + \sum_{s=0}^{+\infty}\frac{2\mu^{2s+1}}{s!}\right|^2 \quad (21)$$

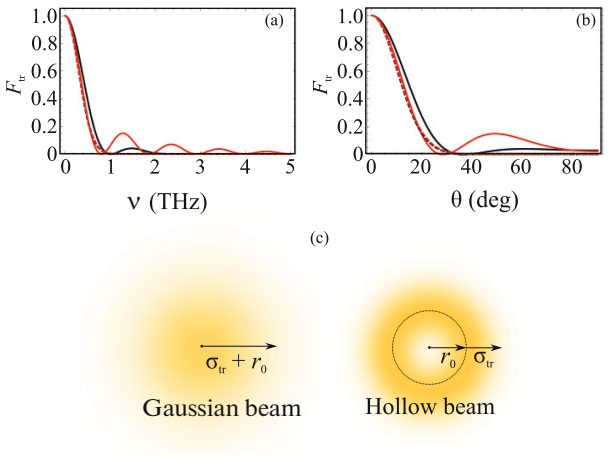

Fig. 5. (Color online) Same as in Fig. 4 but for the Gaussian and hollow beams with the same outer radius.

$$\times\sum_{m=1}^{+\infty}{}_3F_2\left(-m,m,\frac{3}{2}+s;1,\frac{1}{2};1\right)I_m\left[\frac{\sigma_{tr}^2k_{tr}^2}{8}\right]\Bigg|^2.$$

Formula (21) is lengthier than Eq. (16), but it includes the physically informative factor $\exp[-\sigma_{tr}^2k_{tr}^2/4]$, which is useful for the qualitative understanding of the behavior of the solution (e.g., see the asymptotic behavior at high frequencies in Figs. 4a and 5a).

We introduce the radiation observation angles θ and ϕ as follows:

$$n_x = \cos\theta, \quad n_y = \sin\theta\sin\phi, \\ n_z = \sin\theta\cos\phi. \quad (22)$$

It is noteworthy that the determined transverse form factor of the beam depends on the polar angle of radiation observation θ but does not depend on the azimuth angle ϕ. This property is due to the axial symmetry of the beam. If the axial symmetry is broken, e.g., when the electron trajectories in the beam are twisted, the form factor can depend on the angle ϕ. This case requires additional calculations, which are beyond the scope of this work.

To plot the dependences of the form factor (16) on various variables, infinite series should be truncated, e.g., by imposing the condition that the addition of the next terms does not change the plots. It is necessary to take into account that the number of terms depending on the dimensions of the bunch can be rather large.

The dependences of the transverse form factor (16) on the frequency $\nu = \omega/(2\pi)$ and on the polar angle of observation θ are shown by solid lines in Fig. 4 for the beams whose profiles are presented in Fig. 3. It is seen that, as expected, the maximum form factor equal to unity is reached at the smallest observation angles and at the lowest frequencies of radiation. The frequency and angular regions near zero, where the form factor is

close to unity, correspond to the full transverse (spatial) coherence of radiation. These regions are of interest for the development of sources of intense radiation, but they are interesting for the diagnostics of electron bunches only in application to the measurement of longitudinal dimensions. Indeed, the characteristics of radiation in these regions are independent of the transverse dimensions of beams. On one hand, the longitudinal dimensions of the beam cannot be measured; on the other hand, an excess parameter (transverse dimension), which noticeably complicates the solution of the inverse problem to reconstruct the longitudinal dimension/profile of the beam from the measured radiation distribution, is removed.

We now compare the spectral and angular characteristics of the transverse form factor for hollow beams and beams with the Gaussian electron distribution (below, Gaussian beams for brevity).

This comparison is possible in two ways. The first way is to compare the hollow and Gaussian beams with the same standard deviation σ_{tr} (see Fig. 4c). In this case, the transverse electron distribution is given by the same formula (6) with $r_0 = 0$ for the Gaussian beam and $r_0 \neq 0$ for the hollow beam. Then, the form factors of the Gaussian and hollow beams are given by Eqs. (17) and (16), respectively. These form factors are compared in Fig. 4, where dashed lines correspond to the Gaussian beam.

It is seen in Fig. 4 that the form factor of the hollow beam, unlike the Gaussian beam, is an oscillating function of the frequency and polar angle. As a result, a set of particular frequencies are separated in the total radiation intensity. Such a picture is usually observed in the longitudinal form factor (at temporal, i.e., longitudinal, coherence) for periodically modulated beams [23–25]. This additionally allows one to monochromatize the spectrum through the modulation of the hollow beam when the maxima of the longitudinal and transverse form factors are observed at the same frequencies.

It is also seen in Fig. 4 that the region of the full spatial coherence of radiation from the hollow beam is much smaller than that from the Gaussian beam. This means that the effect of transverse dimensions of the beam on the angular and frequency distributions of the radiation intensity can be neglected when processing experimental data for Gaussian beams but cannot be neglected in the case of hollow beams.

The second way of comparison of the spectral and angular characteristics of the transverse form factor for hollow and Gaussian electron beams is possible when the outer radius of the beams is the same, whereas the degrees of population of the inner part of beams by electrons are different (see Fig. 5c). Mathematically, this means that the sum of the radius r_0 and the standard deviation σ_{tr} of the hollow beam is equal to the standard deviation of the Gaussian beam: $\sigma_{tr} + r_0 = \sigma_{tr}^g$. In this case, the transverse form factor of the hollow beam is still given by Eq. (16), whereas Eq. (17) for the Gaussian beam is modified to the form

$$F_{tr} \to \exp(-\sigma_{tr}^2 k_{tr}^2 (\mu + 1)^2/2). \quad (23)$$

The comparison is presented in Fig. 5, where the solid lines for hollow beams are the same as in Fig. 4. According to Fig. 5, the regions of the full spatial coherence of the hollow and Gaussian beams become almost the same because the number of electrons distributed in the same region determined by the outer radius of the bunches is the same.

The population of the inner part of the bunch/beam also strongly affects the form factor at high frequencies and large observation angles in this case: oscillations are observed for the hollow beam and are absent for the Gaussian beam.

4. CONCLUSIONS

It has been shown that the transverse form factor, which is determined by the transverse dimensions of a beam, is important for hollow beams in application to the generation of X-ray photons in free electron X-ray lasers and synchrotrons, including the generation of radiation by electron beams with a nonzero orbital angular momentum. The results are particularly important because the transverse form factor for conventional (not hollow) electron beams is often nearly unity, so that the effect of the transverse dimensions of the beam is neglected.

FUNDING

This study was supported by the Russian Science Foundation (project no. 21-72-00113, D. Sergeeva, Sections 3 and 4) and in part by the Ministry of Science and Higher Education of the Russian Federation (project no. FZWG-2020-0032 (2019-1569), competitive part of the state assignment for the organization and development of laboratories, A. Tishchenko, Sections 1 and 2).

CONFLICT OF INTEREST

The authors declare that they have no conflicts of interest.

REFERENCES

1. G. Stancari, A. Valishev, G. Annala, G. Kuznetsov, V. Shiltsev, D. A. Still, and L. G. Vorobiev, Phys. Rev. Lett. **107**, 084802 (2011).
2. S. Redaelli, R. B. Appleby, R. Bruce, O. Brüning, A. Kolehmainen, G. Ferlin, A. Foussat, M. Giovannozzi, P. Hermes, D. Mirarchi, D. Perini, A. Rossi, and G. Stancari, J. Instrum. **16**, P03042 (2021).
3. X. Gu, W. Fischer, Z. Altinbas, et al., Phys. Rev. Accel. Beams **23**, 031001 (2020).
4. A. Salehilashkajani, H. D. Zhang, M. Ady, et al., Appl. Phys. Lett. **120**, 174101 (2022).
5. C. Behrens, C. Gerth, G. Kube, B. Schmidt, S. Wesch, and M. Yan, Phys. Rev. ST Accel. Beams **15**, 062801 (2012).
6. L. G. Sukhikh, G. Kube, S. Bajt, W. Lauth, Yu. A. Popov, and A. P. Potylitsyn, Phys. Rev. ST Accel. Beams **17**, 112805 (2014).
7. A. Potylitsyn, L. Sukhikh, T. Gusvitskii, G. Kube, and A. Novokshonov, Phys. Rev. Accel. Beams **23**, 042804 (2020).
8. N. Jain, Phys. Plasmas **26**, 023107 (2019).
9. J. Vieira and J. T. Mendonca, Phys. Rev. Lett. **112**, 215001 (2014).
10. N. Jain, T. M. Antonsen, Jr., and J. P. Palastro, Phys. Rev. Lett. **115**, 195001 (2015).
11. I. P. Ivanov and D. V. Karlovets, Phys. Rev. Lett. **110**, 264801 (2013).
12. S. S. Baturin, D. V. Grosman, G. K. Sizykh, and D. V. Karlovets, Phys. Rev. A **106**, 042211 (2022).
13. D. Yu. Sergeeva, A. A. Tishchenko, and M. N. Strikhanov, Nucl. Instrum. Methods Phys. Res., Sect. B **309**, 189 (2013).
14. A. A. Tishchenko and D. Yu. Sergeeva, JETP Lett. **110**, 638 (2019).
15. Y. Shibata, S. Hasebe, K. Ishi, S. Ono, M. Ikezawa, T. Nakazato, M. Oyamada, S. Urasawa, T. Takahashi, T. Matsuyama, K. Kobayashi, and Y. Fujita, Phys. Rev. E **57**, 1061 (1998).
16. Y. Shibata, T. Takahashi, T. Kanai, K. Ishi, and M. Ikezawa, Phys. Rev. E **50**, 1479 (1994).
17. G. P. Williams, C. J. Hirschmugl, E. M. Kneedler, P. Z. Takacs, M. Shleifer, Y. J. Chabal, and F. M. Hoffmann, Phys. Rev. Lett. **62**, 261 (1989).
18. D. Yu. Sergeeva and A. A. Tishchenko, JETP Lett. **115**, 713 (2022).
19. J. S. Nodvick and D. S. Saxon, Phys. Rev. **96**, 180 (1954).
20. G. M. Garibyan and Ya. Shi, *X-Ray Transition Radiation* (Akad. Nauk ArmSSR, Erevan, 1983) [in Russian].
21. I. S. Gradshtein and I. M. Ryzhik, *Tables of Integrals, Series and Products*, 4th ed. (GIFML, Moscow, 1963; Academic, New York, 1980).
22. Y. Luke, Math. Comput. **13**, 261 (1959).
23. D. Y. Sergeeva, A. P. Potylitsyn, A. A. Tishchenko, and M. N. Strikhanov, Opt. Express **25**, 26310 (2017).
24. G. A. Naumenko, A. P. Potylitsyn, D. Yu. Sergeeva, A. A. Tishchenko, M. N. Strikhanov, and V. V. Bleko, JETP Lett. **105**, 553 (2017).
25. G. A. Naumenko, A. P. Potylitsyn, P. V. Karataev, M. A. Shipulya, and V. V. Bleko, JETP Lett. **106**, 127 (2017).

Translated by R. Tyapaev